Available online at www.sciencedirect.com

SCIENCE DIRECT®

Biochimica et Biophysica Acta 1655 (2004) 29–36

BIOCHIMICA ET BIOPHYSICA ACTA

BBA

www.bba-direct.com

Review

Theoretical studies of proton-coupled electron transfer reactions

Sharon Hammes-Schiffer*, Nedialka Iordanova

152 Davey Laboratory, Department of Chemistry, Pennsylvania State University, University Park, PA 16802, USA

Received 23 April 2003; accepted 8 July 2003

Abstract

A theoretical formulation for proton-coupled electron transfer (PCET) is described. This theory allows the calculation of rates and kinetic isotope effects and provides insight into the underlying fundamental principles of PCET reactions. Applications of this theory to PCET reactions in iron bi-imidazoline complexes, oxoruthenium polypyridyl complexes, osmium–benzoquinone systems, amidinium–carboxylate salt bridges, DNA–acrylamide complexes, and ruthenium polypyridyl–tyrosine systems are summarized. The mechanistic insight gained from theoretical calculations on these model systems is relevant to PCET in more complex biological processes such as photosynthesis and respiration.

Keywords: Proton-coupled electron transfer; Hydrogen; Kinetic isotope effect

1. Introduction

Proton-coupled electron transfer (PCET) reactions occur throughout chemistry and biology. The coupling between proton motion and electron transfer plays a vital role in electrochemistry, photosynthesis [1–7], respiration [8,9], and numerous enzyme reactions [10]. A variety of model systems have been investigated experimentally to elucidate the general mechanism of PCET reactions [11–16]. Theoretical calculations [17–32] have assisted in the interpretation of the experimental results and have provided insight into the underlying fundamental principles of PCET.

We have developed a theoretical formulation for PCET that includes both electronic and nuclear quantum effects [20–22]. In this theory, a PCET reaction is described in terms of four charge transfer states, and the transferring hydrogen nucleus is represented as a quantum mechanical wave function. The free energy surfaces are calculated as functions of two collective solvent coordinates corresponding to proton transfer (PT) and electron transfer (ET), respectively. We have derived rate expressions for PCET in various limits [21].

This review outlines the general theoretical formulation for PCET and summarizes the applications of this theory to a wide range of experimentally relevant model systems. The theoretical calculations provide explanations for intriguing experimental observations. For example, the calculations elucidate the basis for experimentally measured trends in rates and kinetic isotope effects. Of particular interest is the relation between single ET and PCET reactions for analogous systems. The calculations also provide insight into the basis for unusually high kinetic isotope effects (i.e., the ratio of the rate with hydrogen to the rate with deuterium) observed in some PCET reactions. The mechanistic insight gained from theoretical calculations on model systems is relevant to PCET in more complex biological processes such as photosynthesis and respiration.

2. Theory of PCET

A single ET reaction may be described in terms of the following two diabatic states:

$$(1)\ D_e^- \quad A_e \qquad (1)$$

$$(2)\ D_e \quad {}^-A_e$$

The free energy surface for a single ET reaction dominated by outer-sphere (solvent) reorganization can be calculated as

* Corresponding author. Tel.: +1-814-865-6442; fax: +1-814-863-5319.

E-mail address: shs@chem.psu.edu (S. Hammes-Schiffer).

0005-2728/$ - see front matter © 2004 Elsevier B.V. All rights reserved.
doi:10.1016/j.bbabio.2003.07.009

a function of a single collective solvent coordinate z_e. The conventional unimolecular rate expression for nonadiabatic ET is [33–36]

$$k^{ET} = \frac{2\pi}{\hbar}|V_{12}|^2(4\pi\lambda k_B T)^{-1/2}\exp\left(\frac{-\Delta G^{\dagger}}{k_B T}\right) \quad (2)$$

where V_{12} is the coupling between the diabatic states, λ is the total reorganization energy, and $\Delta G^{\dagger}$ is the barrier defined as

$$\Delta G^{\dagger} = \frac{(\Delta G^{o} + \lambda)^2}{4\lambda}. \quad (3)$$

This theory of ET has been extended to include the effects of intramolecular solute modes (i.e., inner-sphere reorganization).

The most basic PCET reaction involving the transfer of one electron and one proton may be described in terms of the following four diabatic states:

$$(1a)\ D_e^-\ D_pH\cdots A_p\ A_e \quad (4)$$

$$(1b)\ D_e^-\ D_p^-\cdots {}^+HA_p\ A_e$$

$$(2a)\ D_e\ D_pH\cdots A_p\ A_e^-$$

$$(2b)\ D_e\ D_p^-\cdots {}^+HA_p\ A_e^-$$

where 1 and 2 denote the ET state, and a and b denote the PT state. Within this notation, $1a \rightarrow 1b$ represents PT, $1a \rightarrow 2a$ represents ET, and $1a \rightarrow 2b$ represents EPT (where both the proton and the electron are transferred).

As shown in Ref. [20], the free energy surfaces for PCET reactions may be calculated as functions of two collective solvent coordinates z_p and z_e, corresponding to PT and ET, respectively. Typically the single PT reaction is electronically adiabatic, and often the single ET reaction is electronically nonadiabatic. Here electronically adiabatic refers to reactions occurring in a single electronic state, and electronically nonadiabatic refers to reactions involving multiple electronic states. The electronically adiabatic (or nonadiabatic) limit corresponds to strong (or weak) electronic coupling between the charge transfer states. Even for cases in which the single ET reaction is electronically adiabatic, the overall PCET reaction is usually nonadiabatic because the coupling between the reactant and product vibronic states is small due to averaging over the reactant and product proton vibrational wave functions (i.e., due to the small overlap factor, analogous to the Franck–Condon factor in theories for single ET). In this case, the ET diabatic free energy surfaces corresponding to ET states 1 and 2 are calculated as mixtures of the a and b PT states. The reactants (I) are mixtures of the $1a$ and $1b$ states, and the products (II) are mixtures of the $2a$ and $2b$ states. The proton vibrational states are calculated for both the reactant (I) and product (II) ET diabatic surfaces, resulting in two sets of two-dimensional vibronic free energy surfaces that may be approximated as paraboloids. In this theoretical formulation, the PCET reaction is described in terms of nonadiabatic transitions from the reactant (I) to the product (II) ET diabatic surfaces. Here the ET diabatic states I and II, respectively, may be viewed as the reactant and product PCET states.

The unimolecular rate expression derived in Ref. [21] for PCET is

$$k^{PCET} = \frac{2\pi}{\hbar}\sum_{\mu} P_{1\mu} \sum_{\nu} |V_{\mu\nu}|^2 (4\pi\lambda_{\mu\nu} k_B T)^{-1/2} \exp\left(\frac{-\Delta G^{\dagger}_{\mu\nu}}{k_B T}\right) \quad (5)$$

where $\sum_{\mu}$ and $\sum_{\nu}$ indicate summations over vibrational states associated with ET states 1 and 2, respectively, $P_{1\mu}$ is

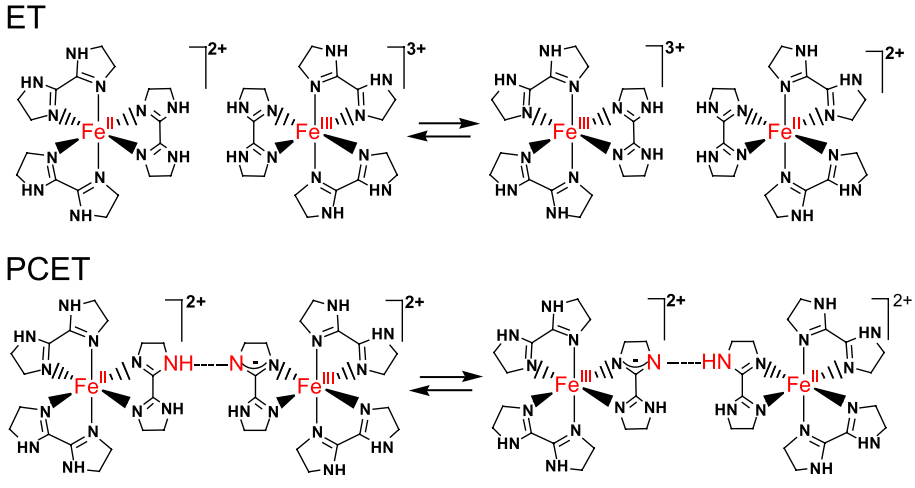

Fig. 1. PCET and single ET reactions between iron bi-imidazoline complexes.

the Boltzmann factor for state Iμ, and

$$\Delta G^{\dagger}_{\mu\nu} = \frac{(\Delta G^{o}_{\mu\nu} + \lambda_{\mu\nu})^2}{4\lambda_{\mu\nu}}. \quad (6)$$

In this expression the free energy difference is defined as

$$\Delta G^{o}_{\mu\nu} = \varepsilon^{II}_{\nu}(\bar{z}^{II\nu}_{p}, \bar{z}^{II\nu}_{e}) - \varepsilon^{I}_{\mu}(\bar{z}^{I\mu}_{p}, \bar{z}^{I\mu}_{e}) \quad (7)$$

where $(\bar{z}^{I\mu}_{p},\bar{z}^{I\mu}_{e})$ and $(\bar{z}^{II\nu}_{p},\bar{z}^{II\nu}_{e})$ are the solvent coordinates for the minima of the ET diabatic free energy surfaces $\varepsilon^{I}_{\mu}(z_p,z_e)$ and $\varepsilon^{II}_{\nu}(z_p,z_e)$, respectively. Moreover, the outer-sphere (solvent) reorganization energy is

$$\lambda_{\mu\nu} = \varepsilon^{I}_{\mu}(\bar{z}^{II\nu}_{p}, \bar{z}^{II\nu}_{e}) - \varepsilon^{I}_{\mu}(\bar{z}^{I\mu}_{p}, \bar{z}^{I\mu}_{e}) = \varepsilon^{II}_{\nu}(\bar{z}^{I\mu}_{p}, \bar{z}^{I\mu}_{e}) - \varepsilon^{II}_{\nu}(\bar{z}^{II\nu}_{p}, \bar{z}^{II\nu}_{e}). \quad (8)$$

The coupling $V_{\mu\nu}$ in the PCET rate expression is defined as

$$V_{\mu\nu} = \langle \phi^{I}_{\mu} \,|\, V(r_p, z^{\dagger}_{p}) \,|\, \phi^{II}_{\nu} \rangle_{p} \quad (9)$$

where the subscript of the angular brackets indicates integration over r_p, $z^{\dagger}_{p}$ is the value of z_p in the intersection region, and ϕ^{I}_{μ} and ϕ^{II}_{ν} are the proton vibrational wave functions for the reactant and product ET diabatic states, respectively. For the systems discussed in this paper,

$$V_{\mu\nu} \approx V^{ET} \langle \phi^{I}_{\mu} \,|\, \phi^{II}_{\nu} \rangle_{p} \quad (10)$$

where V^{ET} is the electronic coupling between states 1*a* and 2*a* and between states 1*b* and 2*b*. The physical basis for this approximation is discussed in Ref. [25]. The effects of inner-sphere solute modes have also been included in this theoretical formulation for several different regimes [21].

The kinetic isotope effects (KIEs) for PCET reactions may be analyzed within the context of the rate expression given in Eq. (5). Each term in this expression represents the rate of a nonadiabatic transition from a reactant to a product state. Based on Eq. (10), the rate for each pair of states is approximately proportional to the square of the overlap between the reactant and product vibrational wave functions. Thus, the KIE for each pair of states is approximately proportional to the square of the ratio of the overlap for hydrogen to the overlap for deuterium. This ratio increases as the vibrational wave function overlap decreases. Moreover, since the vibrational overlap is smallest for the reactive channel involving the lowest energy reactant and product vibrational states, the overall KIE decreases as the contributions from channels involving higher energy vibrational states increase.

Within the framework of this theoretical formulation [20–22], the calculation of the rates and KIEs requires the gas phase valence bond matrix elements and the reorganization energies. The two-dimensional free energy surfaces corresponding to the solvated reactant and product vibronic states are calculated from the gas phase valence bond matrix elements and the solvent reorganization energy matrix elements. The free energy differences $\Delta G^{o}_{\mu\nu}$ and the solvent reorganization energies $\lambda_{\mu\nu}$ are determined from these free energy surfaces, and the couplings $V_{\mu\nu}$ are determined from the associated wave functions and the off-diagonal gas phase valence bond matrix elements (e.g., V^{ET} mentioned above). In practice, the gas phase valence bond matrix elements are represented by molecular mechanical terms

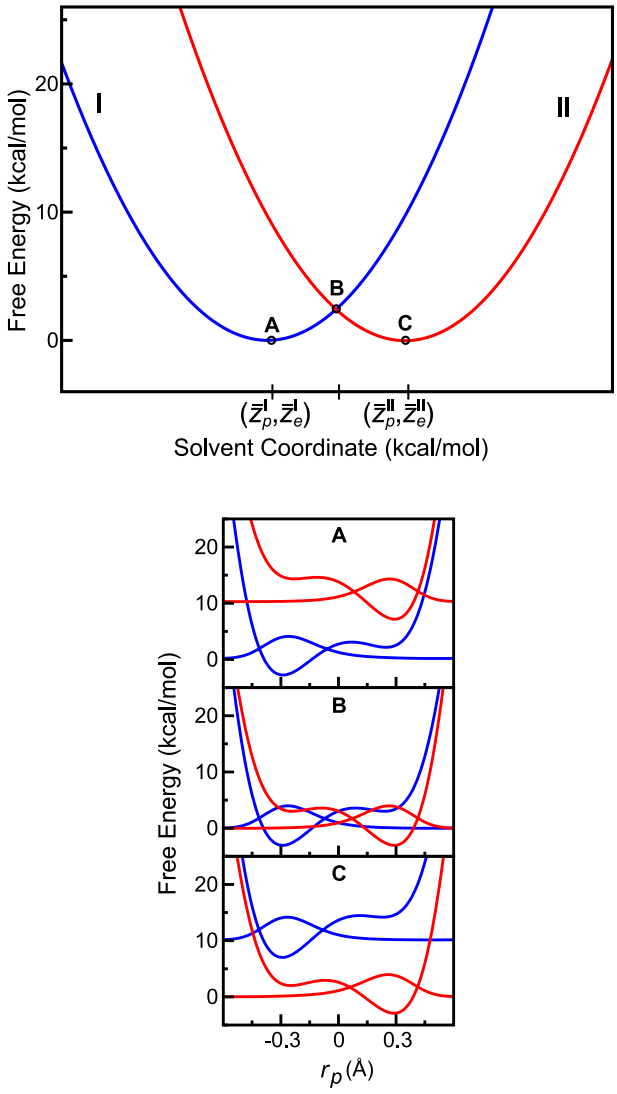

Fig. 2. (a) Slice of the two-dimensional ET diabatic free energy surface along the line connecting the two minima. The lowest energy reactant (I) and product (II) free energy surfaces are shown in blue and red, respectively. Points A, B, and C represent the equilibrium reactant configuration, the intersection point, and the equilibrium product configuration, respectively. (b) Proton potential energy curves and corresponding ground state proton vibrational wave functions as functions of the proton coordinate r_p for the solvent coordinates associated with points A, B, and C indicated in (a). The proton potential energy curves and vibrational wave functions are blue (or red) to denote the reactant (or product) ET diabatic free energy surface [25].

fit to electronic structure calculations or experimental data [37]. The inner-sphere (solute) reorganization energy matrix elements may be calculated from the equilibrium force constants and bond lengths. The outer-sphere (solvent) reorganization energy matrix elements may be calculated with an electrostatic dielectric continuum model or with molecular dynamics simulations including explicit solvent molecules. The applications described in this review were calculated with a multistate continuum theory, in which the solvent was represented as a dielectric continuum.

3. Applications

We have applied the multistate continuum theory [20–22] to a series of PCET reactions. The systems were chosen based on the availability of experimental data that had not yet been fully explained. The results of the theoretical calculations on these systems are summarized in this section. The studies of PCET in iron bi-imidazoline complexes, oxoruthenium polypyridyl complexes, osmium–benzoquinone systems, and ruthenium polypyridyl–tyrosine systems were based on a semiempirical model in which the gas phase valence bond matrix elements were parametrized to fit experimental data. The studies of PCET in thymine–acrylamide complexes and amidinium–carboxylate interface systems were based on a model in which the gas phase valence bond matrix elements were parametrized to fit electronic structure calculations of ground and excited electronic states. In all cases, the solvent was treated as a dielectric continuum [38,39].

A comparative experimental study of single ET and PCET reactions in the iron bi-imidazoline complexes shown in Fig. 1 indicated that the rates of ET and PCET are similar [11]. Previously this result was explained in the context of adiabatic Marcus theory, and the PCET reaction was viewed as a hydrogen atom transfer involving negligible solute charge rearrangement, leading to zero solvent reorganization energy [11]. The similarity of the ET and PCET rates was thought to be due to the compensation of the larger solvent reorganization energy for ET by a larger solute reorganization energy for PCET. The kinetic isotope effect (KIE) for PCET was measured to be a moderate value of 2.3. Our calculations, which were based on nonadiabatic rate expressions for ET and PCET, provided an alternative explanation for the experimental results [25]. The fundamental PCET

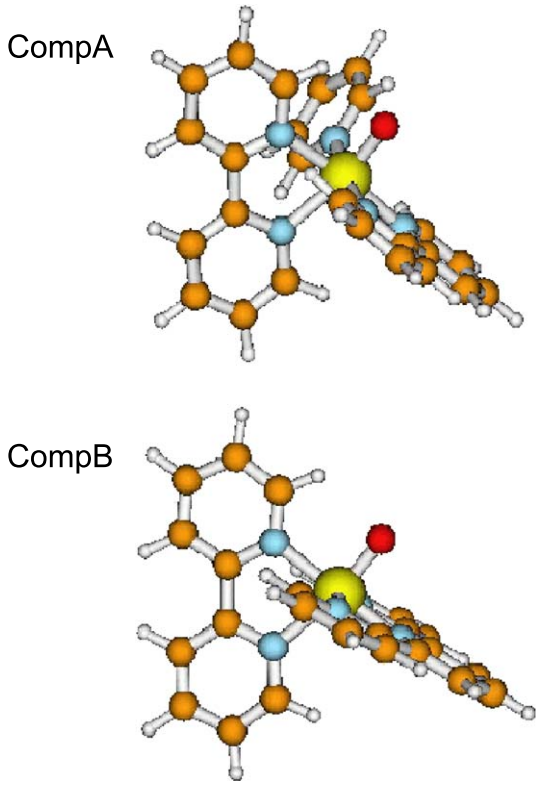

Fig. 4. Structures optimized with density functional theory for the acceptor complexes in Fig. 3 [26].

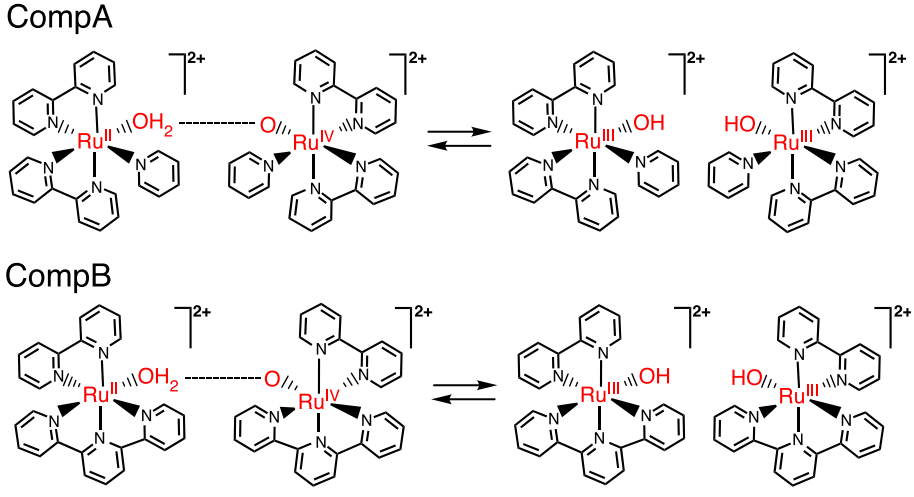

Fig. 3. PCET comproportionation reactions in ruthenium polypyridyl complexes.

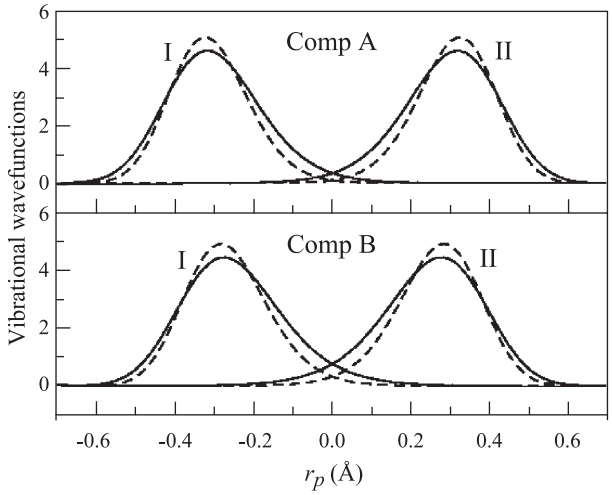

Fig. 5. Reactant (I) and product (II) vibrational wave functions for H (solid) and D (dashed) for the reactions shown in Fig. 3. The overlap is smaller for CompA than for CompB because the O–O distance is larger for CompA due to greater steric crowding near the acceptor oxygen [26].

mechanism for this reaction is illustrated in Fig. 2. In our calculations, the inner-sphere reorganization involving the Fe—N bonds was assumed to be the same for both ET and PCET. The solvent reorganization energies $\lambda_{\mu\nu}$ for the dominant contributions to the PCET reaction were found to be substantial and were $\approx 1-3$ kcal/mol lower than the solvent reorganization energy for single ET. The overall coupling for PCET was found to be smaller than the coupling for ET due to averaging over the reactant and product hydrogen vibrational wave functions (i.e., multiplying by the vibrational overlap factor in Eq. (10)). The calculations indicated that the similarity of the rates for ET and PCET is due mainly to the compensation of the larger solvent reorganization energy for ET by the smaller coupling for PCET. The moderate KIE was determined to arise from the relatively large overlap factor and the significant contributions from excited vibronic states.

An experimental study [12,13] of PCET in the ruthenium polypyridyl complexes shown in Fig. 3 revealed that the CompB rate is nearly one order of magnitude larger than the CompA rate, and the CompA KIE of 16.1 is larger than the CompB KIE of 11.4. As shown in Fig. 4, density functional theory calculations [26] illustrated that the steric crowding near the oxygen proton acceptor is significantly greater for CompA than for CompB. Consistent with this observation, our multistate continuum theory calculations [26] implied that the proton donor–acceptor distance is larger for CompA than for CompB, leading to a larger overlap between the reactant and product hydrogen vibrational wave functions for CompB than for CompA, as shown in Fig. 5. The rate for CompB is larger than the rate for CompA because the rate increases as this overlap factor increases. The KIE for CompB is smaller than the KIE for CompA because the KIE decreases as this overlap factor increases. Both of these KIEs are larger than the KIE for the iron bi-imidazoline complexes described above because the vibrational overlap factor is smaller for the ruthenium systems.

Experimental studies of PCET from a series of osmium complexes to benzoquinone, as shown in Fig. 6, identified unusually high KIEs of up to ~ 400 [15,27]. Our theoretical calculations [40] illustrated that these colossal KIEs arise from the relatively small overlap between the reactant and product hydrogen vibrational wave functions. The KIE increases as the vibrational overlap decreases and as the contribution of transitions between the lowest energy reactant and product vibronic states increases. The trends in the KIEs for a series of osmium complexes were found to be determined by a balance among several factors, including the X–H frequencies and PT distances for the different proton donors (X = N, P, S), as well as the solvent reorganization energies and reaction free energies for the different complexes. These characteristics of the osmium systems influence the overlaps between the reactant and product hydrogen vibrational wave functions and the relative contributions of the excited vibronic states, which in turn impact the KIE.

In addition, this theory has been applied to PCET through amidinium–carboxylate salt bridges, as shown in Fig. 7, where the ET reaction is coupled to the motion of two protons at the PT interface [24]. In this case, the reaction is described in terms of eight valence bond states to include all possible charge transfer states, two hydrogen nuclei are treated quantum mechanically, and the free energy surfaces depend on three solvent coordinates corresponding to the ET and two PT reactions. Experimental studies of photoinduced PCET in analogous systems revealed that the rate for the donor–(amidinium-carboxylate)–acceptor system is substantially slower than the rate for the switched

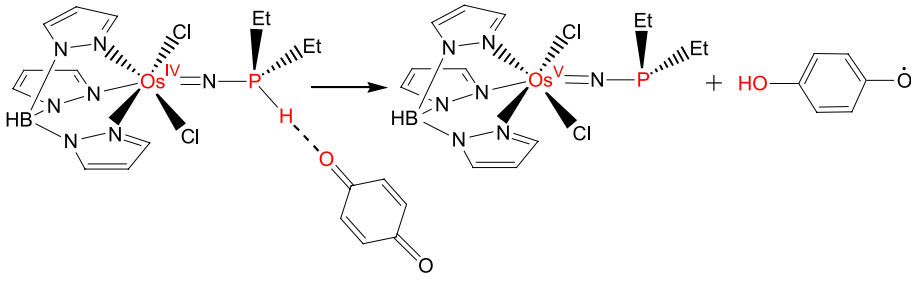

Fig. 6. PCET reaction associated with the reduction of benzoquinone by an osmium complex.

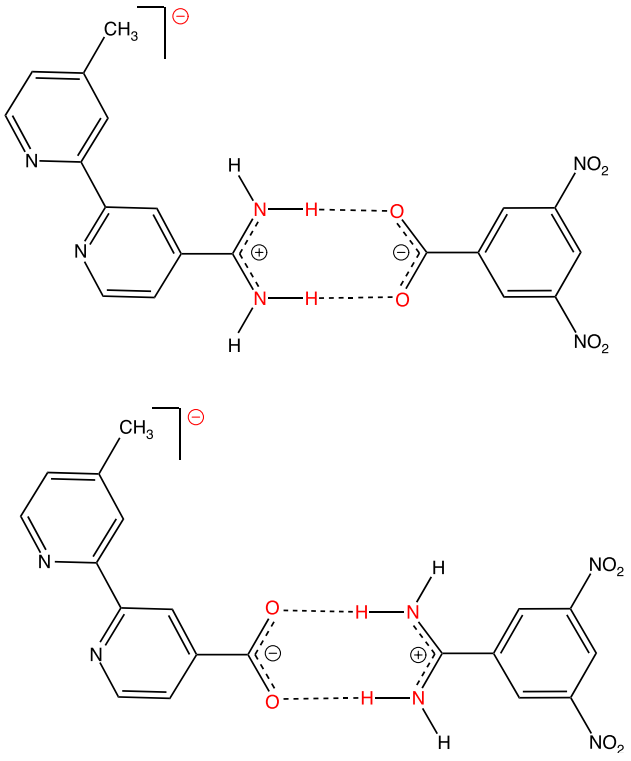

Fig. 7. PCET reactions through an amidinium–carboxylate or carboxylate–amidinium PT interface.

interface donor–(carboxylate-amidinium)–acceptor system [14]. The calculations illustrated that this difference in rates is due mainly to the opposite dipole moments at the PT interfaces for the two systems, leading to an endothermic reaction for the donor–(amidinium-carboxylate)–acceptor system and an exothermic reaction for the switched interface system.

We have also applied this theory to biologically relevant systems, such as PCET in DNA–acrylamide complexes [29]. Experiments implied that PCET may occur in such complexes [41]. The influence of neighboring DNA base pairs was determined theoretically by studying both the solvated thymine–acrylamide complex shown in Fig. 8 and solvated DNA–acrylamide models. The calculations indicated that the final product corresponds to single ET for the solvated thymine–acrylamide complex but to a net

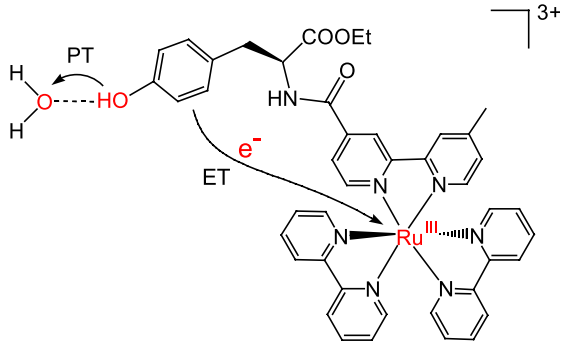

Fig. 9. PCET reaction in a model for tyrosine oxidation in photosystem II. In the first step of the experiment, the ruthenium–tris-bipyridine portion absorbs light, and the excited electron is transferred to an external methyl viologen acceptor. In the second step, which is shown here, the tyrosine portion transfers an electron to the ruthenium and is deprotonated.

PCET reaction for the solvated DNA–acrylamide models. This difference is due to a decrease in solvent accessibility in the presence of DNA, which alters the relative free energies of the ET and PCET product states. Thus, the balance between ET and PCET in the DNA–acrylamide system is highly sensitive to the solvation properties of the system.

Our most recent application [28] of this theory was to the compound depicted in Fig. 9, which was designed to model tyrosine oxidation in Photosystem II [3–7]. In this model system [16], an electron is transferred to the ruthenium from the tyrosine, which is concurrently deprotonated. The dependence of the rates on pH and temperature was measured experimentally [16]. The mechanism was determined to be PCET at pH < 10 when the tyrosine is initially protonated and single ET for pH > 10 when the tyrosine is initially deprotonated. The PCET rate was found to increase monotonically with pH, whereas the single ET rate was found to be independent of pH and two orders of magnitude faster than the PCET rate. The calculations reproduced these experimentally observed trends. The calculations indicated that the larger rate for single ET arises from a combination of factors, including the greater exoergicity for ET, the smaller solvent reorganization energy for ET, and the averaging of the coupling for PCET over the reactant and product hydrogen vibrational wave functions (i.e., the vibrational overlap factor).

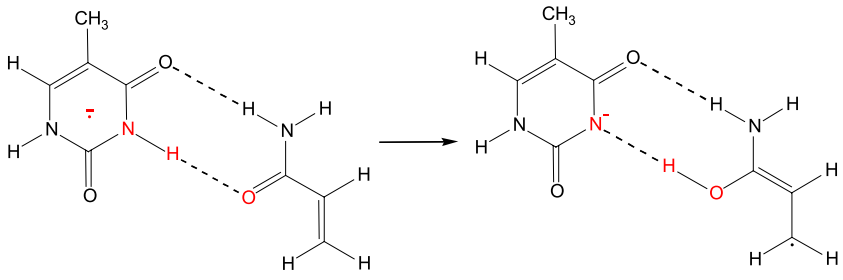

Fig. 8. PCET reaction in the radical anionic thymine–acrylamide complex.

The calculated temperature dependence of the rates and the deuterium kinetic isotope effects were also consistent with the experimental results.

4. Conclusions

This review describes a general theoretical formulation for PCET and summarizes the results of applications to a wide range of model systems. Currently we are extending this theory in several different directions to improve the accuracy and broaden the types of applications. For example, the influence of the proton donor–acceptor vibrational mode has been included to improve the quantitative accuracy and to allow the study of the temperature dependence of PCET rates and kinetic isotope effects in systems such as the enzyme lipoxygenase [42]. The influence of explicit solvent molecules has been investigated for model systems through the development of mixed quantum-classical molecular dynamics methods for PCET reactions [43]. This methodology will be extended to allow the study of PCET in explicit protein environments and to include dynamical effects.

The theoretical calculations described in this review have assisted in the interpretation of experimental data and have provided insight into the underlying fundamental principles of PCET reactions. This synergy between experiment and theory is vital to further progress in the field. The ultimate objective is to elucidate the detailed mechanism of PCET in complex biological processes such as photosynthesis and respiration [1–9].

Acknowledgements

This review is dedicated to Jerry Babcock, whose encouragement and enthusiasm has had a substantial impact on our research. We thank Alexander Soudackov and Claudio Carra for helpful discussions. This work was supported by NSF grant CHE-0096357 and NIH grant GM56207.

References

[1] G.T. Babcock, B.A. Barry, R.J. Debus, C.W. Hoganson, M. Atamian, L. McIntosh, I. Sithole, C.F. Yocum, Water oxidation in photosystem 2: from radical chemistry to multielectron chemistry, Biochemistry 28 (1989) 9557–9565.

[2] M.Y. Okamura, G. Feher, Proton-transfer in reaction centers from photosynthetic bacteria, Annual Reviews of Biochemistry 61 (1992) 861–896.

[3] C. Tommos, X.-S. Tang, K. Warncke, C.W. Hoganson, S. Styring, J. McCracken, B.A. Diner, G.T. Babcock, Spin-density distribution, conformation, and hydrogen bonding of the redox-active tyrosine YZ in photosystem II from multiple electron magnetic-resonance spectroscopies: implications for photosynthetic oxygen evolution, Journal of the American Chemical Society 117 (1995) 10325–10335.

[4] C.W. Hoganson, G.T. Babcock, A metalloradical mechanism for the generation of oxygen from water in photosynthesis, Science 277 (1997) 1953–1956.

[5] C.W. Hoganson, N. Lydakis-Simantiris, X.-S. Tang, C. Tommos, K. Warncke, G.T. Babcock, B.A. Diner, J. McCracken, S. Styring, A hydrogen-atom abstraction model for the function of YZ in photosynthetic osygen evolution, Photosynthesis Research 47 (1995) 177–184.

[6] M.R.A. Blomberg, P.E.M. Siegbahn, S. Styring, G.T. Babcock, B. Akermark, P. Korall, A quantum chemical study of hydrogen abstraction from manganese-coordinated water by a tyrosyl radical: a model for water oxidation in photosystem II, Journal of the American Chemical Society 119 (1997) 8285–8292.

[7] B.A. Diner, G.T. Babcock, in: D.R. Ort, C.F. Yocum (Eds.), Oxygenic Photosynthesis: The Light Reactions, Kluwer Academic Publishing, Dordrecht, The Netherlands, 1996, pp. 213–247.

[8] G.T. Babcock, M. Wikstrom, Oxygen activation and the conservation of energy in cell respiration, Nature 356 (1992) 301–309.

[9] B.G. Malmstrom, Vectorial chemistry in bioenergetics—cytochrome *c* oxidase as a redox-linked proton pump, Accounts of Chemical Research 26 (1993) 332–338.

[10] P.E.M. Siegbahn, L. Eriksson, F. Himo, M. Pavlov, Hydrogen atom transfer in ribonucleotide reductase (RNR), Journal of Physical Chemistry B 102 (1998) 10622–10629.

[11] J.P. Roth, S. Lovel, J.M. Mayer, Intrinsic barriers for electron and hydrogen atom transfer reactions of biomimetic iron complexes, Journal of the American Chemical Society 122 (2000) 5486–5498.

[12] R.A. Binstead, T.J. Meyer, H-atom transfer between metal complex ions in solution, Journal of the American Chemical Society 109 (1987) 3287–3297.

[13] B.T. Farrer, H.H. Thorp, Driving force and isotope dependence of the kinetics of proton-coupled electron transfer in oxoruthenium(IV) polypyridyl complexes, Inorganic Chemistry 38 (1999) 2497–2502.

[14] J.P. Kirby, J.A. Roberts, D.G. Nocera, Significant effect of salt bridges on electron transfer, Journal of the American Chemical Society 119 (1997) 9230–9236.

[15] M.H.V. Huynh, T.J. Meyer, Proton-coupled electron transfer from phosphorus: a P-H/P-D kinetic isotope effect of 178, Angewandte Chemie. International Edition 41 (2002) 1395–1398.

[16] M. Sjodin, S. Styring, B. Akermark, L. Sun, L. Hammarstrom, Proton-coupled electron transfer from tyrosine in a tyrosine–ruthenium–tris-bipyridine complex: comparison with tyrosinez oxidation in photosystem II, Journal of the American Chemical Society 122 (2000) 3932–3936.

[17] R.I. Cukier, Mechanism for proton-coupled electron transfer reactions, Journal of Physical Chemistry 98 (1994) 2377–2381.

[18] R.I. Cukier, Proton-coupled electron transfer reactions: evaluation of rate constants, Journal of Physical Chemistry 100 (1996) 15428–15443.

[19] R.I. Cukier, D.G. Nocera, Proton-coupled electron transfer, Annual Review of Physical Chemistry 49 (1998) 337–369.

[20] A. Soudackov, S. Hammes-Schiffer, Multistate continuum theory for multiple charge transfer reactions in solution, Journal of Chemical Physics 111 (1999) 4672–4687.

[21] A. Soudackov, S. Hammes-Schiffer, Derivation of rate expressions for nonadiabatic proton-coupled electron transfer reactions in solution, Journal of Chemical Physics 113 (2000) 2385–2396.

[22] S. Hammes-Schiffer, Theoretical perspectives on proton-coupled electron transfer reactions, Accounts of Chemical Research 34 (2001) 273–281.

[23] H. Decornez, S. Hammes-Schiffer, Model proton-coupled electron transfer reactions in solution: predictions of rates, mechanisms, and kinetic isotope effects, Journal of Physical Chemistry A 104 (2000) 9370–9384.

[24] I. Rostov, S. Hammes-Schiffer, Theoretical formulation for electron transfer coupled to multiple protons: application to amidinium–carboxylate interface, Journal of Chemical Physics 115 (2001) 285–296.

[25] N. Iordanova, H. Decornez, S. Hammes-Schiffer, Theoretical study of electron, proton, and proton-coupled electron transfer reactions in iron bi-imidazoline complexes, Journal of the American Chemical Society 123 (2001) 3723–3733.
[26] N. Iordanova, S. Hammes-Schiffer, Theoretical investigation of large kinetic isotope effects for proton-coupled electron transfer in ruthenium polypyridyl complexes, Journal of the American Chemical Society 124 (2002) 4848–4856.
[27] M.H. Huynh, T.J. Meyer, personal communication, 2003.
[28] C. Carra, N. Iordanova, S. Hammes-Schiffer, Proton-coupled electron transfer in a model for tyrosine oxidation in photosystem II, Journal of the American Chemical Society 125 (2003) 10429–10436.
[29] C. Carra, N. Iordanova, S. Hammes-Schiffer, Proton-coupled electron transfer in DNA–acrylamide complexes, Journal of Physical Chemistry B 106 (2002) 8415–8421.
[30] J.M. Mayer, D.A. Hrovat, J.L. Thomas, W.T. Borden, Proton-coupled electron transfer versus hydrogen atom transfer in benzyl/toluene, methoxyl/methanol, and phenoxyl/phenol self-exchange reactions, Journal of the American Chemical Society 124 (2002) 11142–11147.
[31] R.I. Cukier, A theory for the rate constant of a dissociative proton-coupled electron transfer reaction, Journal of Physical Chemistry A 103 (1999) 5989–5995.
[32] R.I. Cukier, A theory that connects proton-coupled electron-transfer and hydrogen-atom transfer reactions, Journal of Physical Chemistry B 106 (2002) 1746–1757.
[33] R.A. Marcus, N. Sutin, Electron transfers in chemistry and biology, Biochimica et Biophysica Acta 811 (1985) 265–322.
[34] M. Bixon, J. Jortner, Electron transfer—from isolated molecules to biomolecules, Advances in Chemical Physics 106 (1999) 35–202.
[35] P.F. Barbara, T.J. Meyer, M.A. Ratner, Contemporary issues in electron transfer research, Journal of Physical Chemistry 100 (1996) 13148–13168.
[36] M.D. Newton, N. Sutin, Electron transfer reactions in condensed phases, Annual Review of Physical Chemistry 35 (1984) 437–480.
[37] A. Warshel, Computer Modeling of Chemical Reactions in Enzymes and Solutions, Wiley, New York, 1991.
[38] M.V. Basilevsky, I.V. Rostov, M.D. Newton, A frequency-resolved cavity model (FRCM) for treating equilibrium and non-equilibrium solvation energies, Chemical Physics 232 (1998) 189–199.
[39] M.D. Newton, M.V. Basilevsky, I.V. Rostov, A frequency-resolved cavity model (FRCM) for treating equilibrium and non-equilibrium solvation energies: 2. Evaluation of solvent reorganization energies, Chemical Physics 232 (1998) 201–210.
[40] N. Iordanova, S. Hammes-Schiffer, Colossal Kinetic Isotope Effects for Proton-coupled Electron Transfer Between Osmium Complexes and Benzoquinone, Submittted for publication.
[41] J. Taylor, I. Eliezer, M.D. Sevilla, Proton-assisted electron transfer in irradiated DNA–acrylamide complexes: modeled by theory, Journal of Physical Chemistry B 105 (2001) 1614–1617.
[42] M.J. Knapp, K.W. Rickert, J.P. Klinman, Temperature dependent isotope effects in soybean lipoxygenase: 1. Correlating hydrogen tunneling with protein dynamics, Journal of the American Chemical Society 124 (2002) 3865–3874.
[43] M.N. Kobrak, S. Hammes-Schiffer, Molecular dynamics simulation of proton-coupled electron transfer in solution, Journal of Physical Chemistry B 105 (2001) 10435–10445.